

Determination of the Energy Levels of Radical Pair States in Photosynthetic Models Oriented in Liquid Crystals with Time-Resolved Electron Paramagnetic Resonance

Haim Levanon,^{*,†} Tamar Galili,[†] Ayelet Regev,[†] Gary P. Wiederrecht,[‡] Walter A. Svec,[‡] and Michael R. Wasielewski^{*,‡,§}

Contribution from the Department of Physical Chemistry and The Farkas Center for Light-Induced Processes, The Hebrew University of Jerusalem, Jerusalem 91904, Israel, Chemistry Division, Argonne National Laboratory, Argonne Illinois, 60439-4831, and Department of Chemistry, Northwestern University, Evanston, Illinois 60208-3113

Received February 5, 1998

Abstract: We report the results of time-resolved electron paramagnetic resonance (TREPR) studies of photoinduced charge separation in a series of biomimetic supramolecular compounds dissolved in oriented liquid crystal solvents. The molecules contain a chlorophyll-like (zinc 9-desoxomethylpyropheophorbide *a*) electron donor, D (ZC), and two electron acceptors with different reduction potentials, i.e., pyromellitimide, A₁ (PI), and 1,8:4,5-naphthalenediimide, A₂ (NI). The compounds investigated are ZCPI, ZCNI, and ZCPINI, and they have small but well-defined differences of their ion-pair energies. Temperature-dependent TREPR studies on this series of compounds permit the determination of the radical pair energy levels as the solvent reorganization energy increases from the low-temperature crystalline phase, through the soft glass phase, to the nematic phase of the liquid crystal. As the temperature is increased, the radical pair with the lowest energy is the first to exhibit triplet-initiated charge separation as the solvent reorganization energy increases in the liquid crystal. The energy levels of the radical pairs and the solvent reorganization energy are determined by using the known singlet and triplet excited state energy levels of ZC, the electrochemically determined relative energies between the radical ion pairs in polar isotropic solvents, and the TREPR data. All these yield information about the ordering of the radical ion pair energy levels relative to the excited-state energy levels of ZC.

Introduction

It is well recognized that singlet photochemistry governs charge separation in natural photosynthesis (PS), while in model systems, both singlet and triplet channels are competitive and depend on several variables such as relative orientations, distances, and electronic couplings between the participating redox partners.¹ In addition, the solvent reorganization energy (λ_s) due to solvent dipoles reorienting around the ion pair is of prime importance for tuning the energy levels of the charge-separated states, such that the branching ratio of the electron transfer rates, i.e., singlet- or triplet-initiated routes, can be controlled. Thus, to achieve the goal of mimicking natural PS by biomimetic supramolecular systems, it is essential to develop experimental methods to explicitly determine the energy levels of radical ion pair (RP) states. We show that this goal can be achieved by blending together molecular architecture, solvent properties, and fast EPR detection of paramagnetic transients.

Recent studies of intramolecular electron transfer (IET) illustrate the unique properties of liquid crystals (LCs) that make

them interesting solvents in which to study covalently linked donor–spacer–acceptor systems.^{2–5} Most importantly, the IET rates in these solvents are reduced by several orders of magnitude (from ps to ns), permitting the observation of IET processes on submicrosecond time scales with time-resolved electron paramagnetic resonance (TREPR) spectroscopy.² This reduction of IET rates is due to the nematic potential associated with the alignment of the LC molecules, which restricts the isotropic molecular reorientation found in conventional solvents.^{2,6,7} These inherent properties of LCs permit tuning the RP states into a time domain where the paramagnetic transients can be monitored over a wide temperature range.^{2,8}

The powerful approach of coupling TREPR with LC solvents has permitted the elucidation of photochemical mechanisms that otherwise could not be observed. In particular, this technique recently permitted the first observation of the special spin-polarized triplet excited state in a multicomponent model system generated by the same mechanism of back electron transfer observed in natural PS.^{9,10} It is noteworthy that this model

[†] The Hebrew University of Jerusalem.

[‡] Argonne National Laboratory.

[§] Northwestern University.

(1) Joran, A. D.; Leland, B. A.; Felker, P. M.; Zewail, A. H.; Hopfield, J. J.; Dervan, P. B. *Nature* **1987**, 327, 508.

(2) For a general review see, e.g.: Levanon, H.; Hasharoni, K. *Prog. React. Kinet.* **1995**, 20, 309.

(3) Greenfield, S. R.; Svec, W. A.; Wasielewski, M. R.; Hasharoni, K.; Levanon, H. In *The Reaction Center of Photosynthetic Bacteria*; Michel-Beyerle, M.-E., Ed.; Springer: Berlin, 1996; pp 81–87.

(4) Wiederrecht, G. P.; Svec, W. A.; Wasielewski, M. R. *J. Am. Chem. Soc.* **1997**, 119, 6199.

(5) van der Est, A.; Fuechsle, G.; Stehlik, D.; Wasielewski, M. R. *Appl. Magn. Reson.* **1997**, 13, 317.

(6) Meier, G.; Saupe, A. *Mol. Cryst.* **1966**, 1, 515.

(7) Martin, A. J.; Meier, G.; Saupe, A. *Symp. Faraday Soc.* **1971**, 5, 119.

(8) Hasharoni, K.; Levanon, H. *J. Phys. Chem. A* **1995**, 99, 4875.

(9) Hasharoni, K.; Levanon, H.; Greenfield, S. R.; Gosztola, D. J.; Svec, W. A.; Wasielewski, M. R. *J. Am. Chem. Soc.* **1995**, 117, 8055.

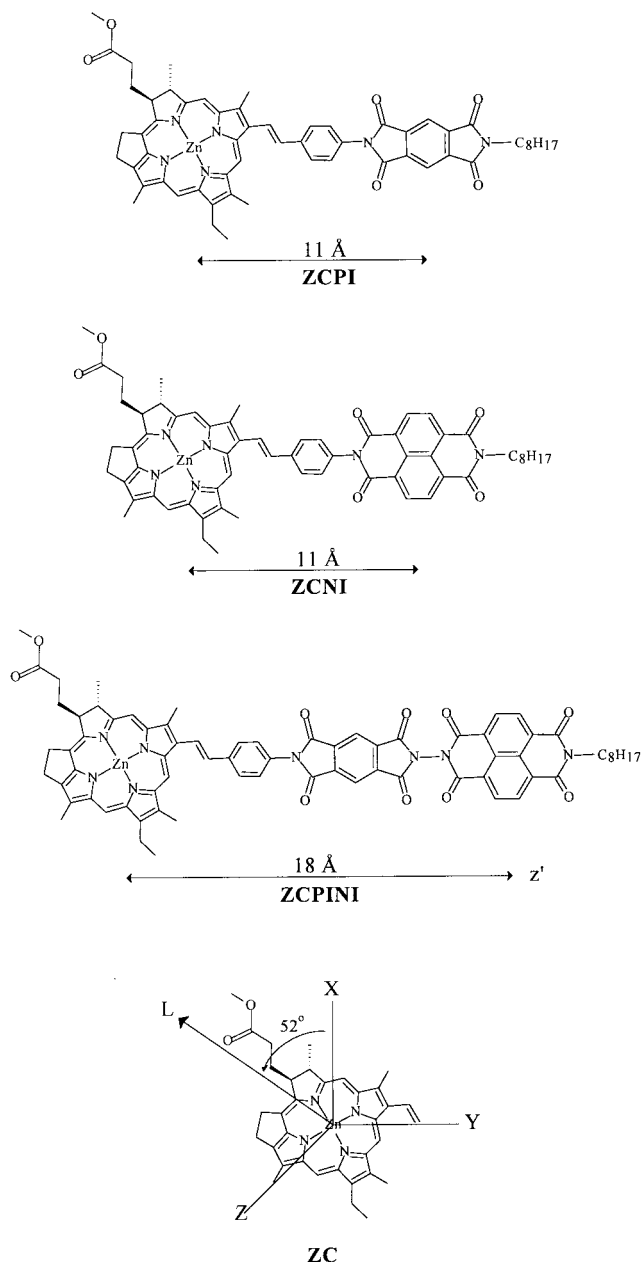


Figure 1. Schematic structures of the donor-acceptor systems. For ZC, the molecular frame of reference is shown. The angle $\phi = 52^\circ$ between L and the X-axis was obtained via the spectral simulations. This value is expected by examining the molecular structure. The z'-axis is the dipolar axis between the donor and the acceptor (common to all three molecules).

system consists of non-porphyrinoid entities, and further studies of multistep ET processes within porphyrinoid systems dissolved in LCs would be valuable.

The present paper deals with a series of covalently linked compounds (Figure 1) containing a chlorophyll-like (chlorin) electron donor, D (ZC). Two electron acceptors are used with different reduction potentials, i.e., pyromellitimide, A₁ (PI), and 1,8:4,5-naphthalenediimide, A₂ (NI), to produce a series of molecules with small but well-defined differences of the ion-pair energies. The compounds investigated are ZCPI, ZCNI, and ZCPINI, with D-to-A₁, D-to-A₂ and D-to-A₂ center-to-center distances of ~11, ~11, and ~18 Å, respectively¹¹ (for conciseness the spacer is not mentioned in the acronyms). These

(10) Hasharoni, K.; Levanon, H.; Greenfield, S. R.; Gosztola, D. J.; Svec, W. A.; Wasielewski, M. R. *J. Am. Chem. Soc.* **1996**, *118*, 10228.

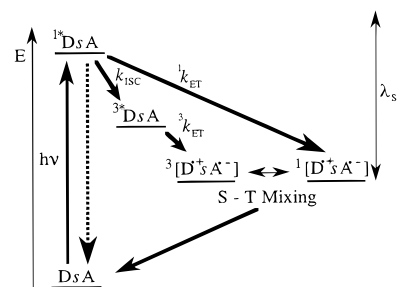


Figure 2. Energy level diagram of the IET reactions, valid for all donor-spacer-acceptor molecules. The solvent reorganization energy, which is temperature dependent, is represented schematically by λ_s .

compounds, when oriented in different LCs, undergo photo-induced IET to produce charge-separated states that can be monitored by TREPR. The origin of such states and the spin dynamics associated with them strongly depend not only on λ_s , but also very substantially on the molecular architecture. Thus, the short donor-acceptor distances in ZC⁺-PI⁻ and ZC⁺-NI⁻, may lead to a relatively large singlet (S)-triplet (T₀) separation. Under such conditions, the observed spectrum is typical of a triplet radical pair (TRP), i.e., ³[D⁺-A⁻], with a negative zero-field splitting (ZFS) parameter, *D*, due to "head-to-tail" spin alignment.² On the other hand, the longer donor-acceptor distance in the triad, ZC⁺-PI-NI⁻, may result in a correlated radical pair (CRP) spectrum, i.e., ^{1,3}[D⁺-A₁-A₂⁻], due to S-T₀ mixing in a four-level system.² As will be discussed in detail below, these two types of spectra can be differentiated only by TREPR, via the dipolar and/or the exchange interactions, which strongly depend on the donor-acceptor distance. We further show that the spectral analysis in terms of the different pathways of triplet excited state and RP state production, illustrated in Figure 2, permits an accurate assignment of the energies of the RPs in the different phases of the LC solvents. This is the first demonstration of RP energy level determination for short-lived RPs by tuning, via temperature change, the solvent reorganization energy (λ_s) through the different LC phases.

Experimental Section

The syntheses of the novel triad system zinc methyl 13¹-desoxyprophoeophorbide *a* - pyromellitimide-1,8:4,5-naphthalenediimide (ZCPINI) as well as the dyad control molecules ZCPI and ZCNI are described elsewhere.¹¹ TREPR (CW) measurements were performed on ZCPINI, ZCPI, ZCNI, and ZC, utilizing two liquid crystal solvents (Merck Ltd.) with different dielectric constants (E-7, $\epsilon = 19.0$; ZLI-1167, $\epsilon = 7.5$).¹² The compounds were first dissolved in toluene (~1 mM) in 4 mm OD pyrex tubes, and after evaporating the solvent the LC was introduced. All samples were degassed by several freeze-pump-thaw cycles on a vacuum line. The temperature was maintained by using a variable-temperature nitrogen flow dewar in the EPR resonator. Samples were excited at 640 nm (20 mJ/pulse at a repetition rate of 20 Hz) by a dye laser (Continuum, TDL-60) pumped by the second harmonic of a Nd:Yag laser (Continuum, 661-20). This wavelength corresponds to the Q-band absorption of the chlorin (ZC) moiety. TREPR measurements were carried out on a Varian E-12 with the field modulation disconnected. The EPR signal was taken from a preamplifier connected directly to the microwave diode detector. The signal was amplified and fed into a backoff amplifier and finally into

(11) Wiederrecht, G. P.; Niemczyk, M. P.; Svec, W. A.; Wasielewski, M. R. *J. Am. Chem. Soc.* **1996**, *118*, 81.

(12) The chemical compositions are as follows: E-7 is an eutectic mixture of R₁-C₆H₅-C₆H₅-CN where R₁ = C₃H₁₁ (51%), R₂ = C₇H₁₅ (25%), R₃ = C₈H₁₇O (16%), and R₄ = C₅H₁₁C₆H₅ (8%); ZLI-1167 is an eutectic mixture of R'₁-C₆H₁₀-C₆H₁₀-CN where R'₁ = C₃H₇, R'₂ = C₅H₁₁, and R'₃ = C₇H₁₅.

Table 1. Triplet Parameters of the Compounds ${}^3\text{ZCX}$ Studied in the Various Media

molecule	medium	T (K)	$ D ^a$	$ E ^a$	$A_x:A_y:A_z$
ZC	E-7	143	319	60	0.03:0.15:0.82
ZCPI	E-7	129	322	63	0.05:0.15:0.80
ZCNI	E-7	141	322	63	0.05:0.15:0.80
ZCPINI	E-7	138	322	63	0.05:0.15:0.80

^a Units: $\times 10^4 \text{ cm}^{-1}$. Estimated errors ± 5 .**Table 2.** Parameters of the TRP Dyads, ${}^3[\text{ZC}^{*+}-\text{X}^-]^a$

molecule	medium	T (K)	D^b	$ E ^b$	$A_x:A_y:A_z$
ZCPI	E-7	303	-16.8	1.9	0.80:0.05:0.15
ZCNI	E-7	303	-16.8	1.4	0.80:0.05:0.15
ZCNI	ZLI-1167	323	-16.8	1.4	0.80:0.05:0.15

^a The triad is not shown, because its line shape is governed by the CRP mechanism. ^b Units: $\times 10^4 \text{ cm}^{-1}$. Estimated errors ± 0.5 .

a digital oscilloscope. The time resolution in the diode-detected mode was ~ 200 ns. The spectra at different times after the laser pulse with respect to the external magnetic field were reconstructed from kinetic traces for each field position. The samples dissolved in LCs were aligned in the microwave cavity by first warming them in the nitrogen flow system to the temperatures above the clearing point of the LCs in a high magnetic field (10 kG) for 10 min and then cooled to the desired temperature.

During the experiment, two sample orientations were studied, $\mathbf{L} \parallel \mathbf{B}$ and $\mathbf{L} \perp \mathbf{B}$, where \mathbf{L} is the director of the LC. The sign of the diamagnetic susceptibility ($\Delta\chi$) determines the relationship between \mathbf{L} and \mathbf{B} in the nematic phase, i.e., $\Delta\chi = \chi_{\parallel} - \chi_{\perp}$. A positive $\Delta\chi$ causes the initial alignment to be $\mathbf{L} \parallel \mathbf{B}$, which is the case for E-7. A negative $\Delta\chi$ leads to an $\mathbf{L} \perp \mathbf{B}$ initial alignment, which is the case for ZLI-1167. A LC characterized by a negative $\Delta\chi$ is also referred to as a "multidomain" configuration, due to the fanning of the directors of the LC in the plane perpendicular to \mathbf{B} . Spectra for $\mathbf{L} \perp \mathbf{B}$ in E-7 can also be obtained when the sample is held below the freezing temperature. These spectra are obtained by rotation of the sample in the microwave cavity by $\pi/2$ about an axis perpendicular to the external magnetic field. However, in the fluid nematic phase, rotation of the sample from the $\mathbf{L} \parallel \mathbf{B}$ position does not affect the spectral line shape due to molecular reorientation back to the initial parallel orientation.

The phase diagram of a nematic LC (e.g., E-7) exhibits three distinct phases with well-defined transition temperatures. Qualitatively, we define an additional phase, referred to as the soft glass (SG), which is found at higher temperatures within the crystalline phase. This regime is characterized by limited molecular motion. This phenomenon has been previously observed in other TREPR experiments in frozen LCs.² The other LC, ZLI-1167, does not exhibit the soft glass characteristics of E-7, but exhibits an additional smectic phase. The reason for employing this LC is to differentiate between the spin polarization mechanisms that are operative using the donor-acceptor systems studied here. The phase transition temperatures for both LCs are

E-7: crystalline $\xrightarrow{210 \text{ K}}$ soft glass $\xrightarrow{263 \text{ K}}$ nematic $\xrightarrow{333 \text{ K}}$ isotropic

ZLI-1167: crystalline $\xrightarrow{287 \text{ K}}$ smectic $\xrightarrow{305 \text{ K}}$ nematic $\xrightarrow{356 \text{ K}}$ isotropic

Line shape analyses of the triplet EPR spectra of ${}^3\text{ZC}$, ${}^3\text{ZCX}$, and ${}^3[\text{ZC}^{*+}-\text{X}^-]$, where $\text{X} = \text{PI}, \text{NI},$ or PINI , were carried out for uniaxial ($\Delta\chi > 0$) and multidomain ($\Delta\chi < 0$) LCs as described elsewhere in detail.^{13,14} The extracted ZFS parameters, D and E , and the corresponding relative triplet population rates, A_x , A_y , and A_z , are given in Tables 1 and 2. In the triplets, ${}^3\text{ZC}$ and ${}^3\text{ZCX}$, the canonical

Table 3. The Reduction Potentials of PI and NI in Benzonitrile vs SCE; the Free Energies of Charge Separation and RP Energies Calculated for Isotropic E-7

molecule	E_{RED} (eV)	r_{12} (Å)	ΔG_{CS} (eV)	E_{RP} (eV)
$\text{ZC}^{*+}-\text{PI}^-$	-0.87	11	-0.72	1.23
$\text{ZC}^{*+}-\text{NI}^-$	-0.60	11	-0.99	0.96
$\text{ZC}^{*+}-\text{PI}-\text{NI}^-$	-0.41	18	-1.15	0.8

orientations associated with the out-of-plane Z -axis of the porphyrin moiety was found to be, as expected by previous studies, preferentially populated.¹⁵

Further experimental procedures were utilized to verify the TREPR results. These include transient pump-probe spectroscopy and fluorescence quenching experiments. The pump-probe spectroscopy was performed utilizing an amplified Ti:sapphire system that pumps an optical parametric amplifier. The system has been described in detail elsewhere.¹⁶ Optical excitation at 638 nm selectively pumps the Q_y -band of the chlorin electron donor, and intramolecular electron-transfer results. These molecules are ideal for pump-probe experiments since the radical anions have distinct and narrow absorption bands at 720 nm for PI^- and 480 nm for NI^- .¹¹ The spectral characteristics of the anions provide unambiguous proof that intramolecular charge separation has occurred. However, high optical quality media are generally required for this technique, so that a solvent that produces an optical quality glass at low temperatures, such as methyltetrahydrofuran (MTHF) or toluene, is required. While the stiff, glassy state of MTHF at 77 K is probably a good mimic for the lack of solvent motion in crystalline frozen LCs, we also performed fluorescence quenching measurements (Photon Technology International-1738 fluorimeter) at low temperatures for ZCX in the LCs themselves to verify that charge separation was in fact occurring. In these experiments the fluorescence of ZCX was monitored at 650 nm and compared to that of ZC alone to determine the magnitude of quenching due to electron transfer. The redox potentials for ZCPI, ZCNI, and ZCPINI were determined in benzonitrile/0.1 M tetra-*n*-butylammonium perchlorate at a Pt electrode referenced to a saturated calomel electrode (SCE) with cyclic voltammetry.

Results and Discussion

Electrochemical Data. The electrochemical data presented in Table 3 are used to estimate the free energies for photoinduced charge separation (ΔG_{CS}) and thermal recombination of the RPs (ΔG_{CR}) for ZCPI, ZCNI, and ZCPINI in the isotropic phase of E-7, as calculated from the following equations:^{17,18}

$$\Delta G_{\text{CS}} = E_{\text{OX}} - E_{\text{RED}} - e_0^2/\epsilon_s r_{12} - E_s \quad (1)$$

$$\Delta G_{\text{CR}} = -\Delta G_{\text{CS}} - E_s = -E_{\text{RP}} \quad (2)$$

Here, $E_s = 1.95$ eV is the first excited singlet-state energy of the donor chromophore, $E_{\text{OX}} = 0.43$ V is the oxidation potential of the electron donor, E_{RED} is the reduction potential of the electron acceptor, e_0 is the electronic charge, ϵ_s is the static dielectric constant, and r_{12} is the center-to-center distance between the donor and acceptor. The ΔG_{CS} and E_{RP} values for the donor-acceptor molecules dissolved in isotropic E-7 were calculated by using $\epsilon_s = 19$.^{11,19} The data show that ΔG_{CS} for

(15) Levanon, H.; Norris, J. R. In *Light Reaction Path of Photosynthesis*; Fong, F. K., Ed.; Springer-Verlag: Berlin, 1982; pp 152-195.

(16) Greenfield, S. R.; Wasielewski, M. R. *Appl. Opt.* **1995**, *34*, 2688.

(17) Wasielewski, M. R. *Chem. Rev.* **1992**, *92*, 435.

(18) Wasielewski, M. R.; Gaines, G. L., III; O'Neil, M. P.; Svec, W. A.; Niemczyk, M. P.; Prodi, L.; Gosztola, D. In *Dynamics and mechanics of photoinduced transfer and related phenomena*; Mataga, N., Okada, T., Masuhara, H., Eds.; Elsevier: New York, 1992; p 87.

(19) For ZLI-1167 $\epsilon_s = 7.5$, thus, 0.1 eV should be added to the values for ΔG_{CS} and 0.1 eV subtracted from the values for ΔG_{CR} . Nevertheless, it is easy to show that the change in the gap between two different solvents is negligible.

(13) Gonen, O.; Levanon, H. *J. Chem. Phys.* **1986**, *84*, 4132.

(14) Regev, A.; Galili, T.; Levanon, H. *J. Phys. Chem. A* **1996**, *100*, 18502.

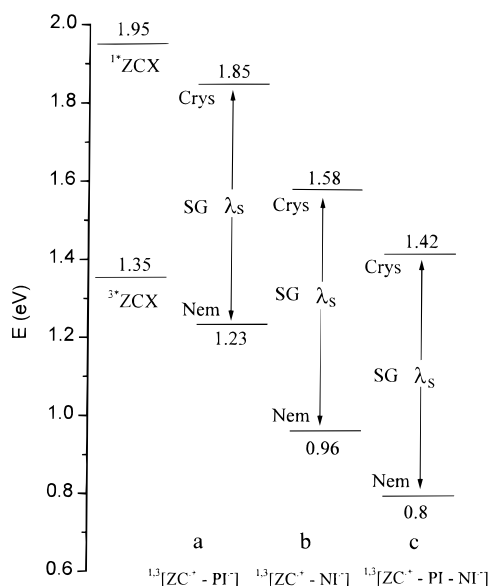


Figure 3. The energy levels of the three RPs determined by TREPR data are shown. The energy levels of the RPs within the crystalline (Crys) and nematic (Nem) phases bracket the distribution of the RP energies throughout the temperature range of the soft glass (SG) phase. The energy level difference between the glass and nematic phases is reflected by the reorganization energy of E-7: (a) ZCPI; (b) ZCNI; and (c) ZCPINI. The given values are accurate to ± 0.1 eV.

singlet-initiated charge separation is most negative for ZCPINI followed by ZCNI and ZCPI. Note, however, that the ΔG_{CS} for production of $ZC^{\bullet+}-PI-NI^{\bullet-}$ vs $ZC^{\bullet+}-NI^{\bullet-}$ are different. This is a consequence of the fact that the NI acceptor is more easily reduced by 0.19 eV when coupled to PI, leading to a considerably larger driving force for photoinduced charge separation, which results in a faster rate of charge separation within the triad than within the dyads.¹¹

Strictly speaking, eq 1 is valid only in polar isotropic liquids where the solvent dipoles are free to reorient in the presence of a RP.¹⁸ As a result, RP energies in low-polarity solvents or in crystalline and stiff, glassy environments are difficult to calculate accurately. The magnitude of this destabilization produces uncertainty about the absolute value of the RP energies. Recent work with a variety of porphyrin model systems indicates that the RPs are destabilized by approximately 0.8 eV in MTHF glass at 77 K relative to the fluid solvent at room temperature.¹⁸ We show here that the use of a combination of TREPR and electrochemical data permits the determination of the energy levels of the RPs in a closely related series of donor-acceptor molecules with reasonable precision. The assignment of these energy levels is based on knowledge of three types of information. First, the singlet and triplet excited-state energy levels of the ZC donor are known and remain constant within the series of molecules under study. Second, the appearance of the triplet excited state, 3ZC , and/or the triplet/singlet initiated RPs, $^{1,3}(D^{\bullet+}-A^{\bullet-})$ observed by TREPR is determined by the ordering of the energy levels of these states. Third, the relative values between the energies of the RP states are determined by the electrochemical data for the donors and acceptors obtained in polar media given in Table 3. These relative energy levels are assumed to be only weakly solvent dependent. The results of our studies are summarized in Figure 3 and Table 4 for the RPs in LCs.

Time-Resolved EPR of ZCPI, ZCNI, and ZCPINI. (a) Crystalline and Stiff Glass Phases. All three compounds exhibit a triplet excited-state spectrum (3ZCX) in the low-

temperature crystalline phase of E-7, while RP spectra are only observed for $ZC^{\bullet+}-PI-NI^{\bullet-}$ and $ZC^{\bullet+}-NI^{\bullet-}$. No spectrum attributable to $ZC^{\bullet+}-PI^{\bullet-}$ was observed at these low temperatures. Although TREPR data do not indicate the presence of a radical pair for ZCPI in the crystalline phase, fluorescence quenching measurements and transient pump-probe spectroscopy both indicate that the RP is formed. The fluorescence quantum yield of ZC within ZCPI at 650 nm is quenched by more than a factor of 30 relative to that of ZC in the crystalline phase of the LC. Transient pump-probe spectroscopy was performed on ZCPI dissolved in both MTHF (77 K) and toluene glasses (120 K). These solvents were substituted for the LC because crystallization of the LC results in a highly scattering medium that prevents the transmission of the probe beam through the sample. At low temperatures the motion of the solvent in both the LC and in glassy MTHF and toluene should be highly restricted. In both MTHF and toluene the distinct absorption band of $PI^{\bullet-}$ at 720 nm was observed with a charge separation time of approximately 2 ps and a charge recombination time of 50 ps. Thus, charge separation occurs in the stiff, glassy phase of these solvents with near unity quantum yield. Given the results of the fluorescence quenching and pump-probe measurements for ZCPI, it is reasonable to conclude that charge separation does occur. The absence of a TREPR signal is most likely due to the short lifetime of the $ZC^{\bullet+}-PI^{\bullet-}$ radical pair in the LC.

The TREPR data in crystalline E-7 are consistent with the driving forces for charge separation of the order given in Table 3, i.e., $ZC^{\bullet+}-PI-NI^{\bullet-} > ZC^{\bullet+}-NI^{\bullet-} > ZC^{\bullet+}-PI^{\bullet-}$. In further support for this argument, the EPR data indicate that the RP states of $ZC^{\bullet+}-NI^{\bullet-}$ (exhibiting a weak EPR spectrum) and $ZC^{\bullet+}-PI-NI^{\bullet-}$ are not formed via a triplet-initiated route (Table 4). In other words, the RP energy levels all lie below that of the 1ZCX state and above the 3ZCX energy level. Moreover, the RP signal of $ZC^{\bullet+}-PI-NI^{\bullet-}$ shows no correlation between its formation and the decay of the triplet precursor, 3ZCX (Table 4). The lack of such a correlation indicates that the singlet-initiated route is the active one.

Since the energy levels of the three radical pairs lie between the singlet and triplet excited state energy levels of ZCX in the crystalline LC phase, reasonable quantitative determination of the RP energy levels is possible. The relative energy levels of the three RPs span 0.43 eV as shown in Table 3. Furthermore, these three energy levels must lie within a 0.6 eV range as determined by the difference in the singlet and triplet energy levels of ZCX. Placing the RP energy levels approximately in the center of this range gives a value of 1.85 eV for $ZC^{\bullet+}-PI^{\bullet-}$, 1.58 eV for $ZC^{\bullet+}-NI^{\bullet-}$, and 1.42 eV for $ZC^{\bullet+}-PI-NI^{\bullet-}$, with error bars of ± 0.1 eV. These values indicate that the RPs are destabilized in the crystalline phase of LCs by approximately 0.6 eV relative to an isotropic solvent. The RP energy levels are illustrated in Figure 3.

An additional spectral parameter, which is of substantial importance for understanding the spin dynamics, is the phase inversion of the time-evolved EPR spectra. Phase inversion usually indicates the participation of two IET routes, e.g., a singlet-initiated RP that can be accompanied by a triplet-initiated RP.¹⁰ The spectrum of the triplet-initiated RP starts to appear at later times. At these low temperatures the TREPR spectrum of $ZC^{\bullet+}-PI-NI^{\bullet-}$ (not shown) does not exhibit a phase inversion with respect to time. This immediately suggests that even for the case of the lowest energy RP (Figure 3), the energy

Table 4. Kinetic Data Based on Eq 5^a

molecule	phase	<i>T</i> (K)	medium	τ_{RSRP}	τ_{RTRP}	τ_{DRP}	τ_{RT}	τ_{DT}	phase (RP)
ZCPI	crystalline	133	E-7				0.36	0.67	
ZCPI	SG ^b	250	E-7	1.0	1.4	9.6	0.32	1.1	a/e → e/a ^c
ZCPI	nematic	300	E-7	0.42	<i>d</i>	0.50			a/e → e/a ^c
ZCPI	smectic	299	ZLI-1167	0.38		0.53			a/e
ZCPI	nematic	323	ZLI-1167	0.34	<i>d</i>	0.46			a/e → e/a ^c
ZCNI	crystalline	133	E-7	<i>d</i>		<i>d</i>	0.23	1.1	
ZCNI	SG ^b	240	E-7	0.38	0.60	6.0	0.26	1.0	a/e → e/a ^c
ZCNI	nematic	299	E-7	0.20	0.22	0.22			a/e → e/a ^c
ZCNI	smectic	299	ZLI-1167	0.13	0.19	0.23			a/e → e/a ^c
ZCNI	nematic	323	ZLI-1167	0.13	0.16	0.22			a/e → e/a ^c
ZCPINI	crystalline	136	E-7	0.23		0.36	0.28	1.5	(e/a) ; (a/e) _⊥
ZCPINI	SG ^b	240	E-7	0.18	0.32	5.4			e/a → a/e ^c
ZCPINI	nematic	300	E-7		0.37	2.03			a/e
ZCPINI	nematic	315	ZLI-1167	0.26	0.31	1.4			a/e → e/a ^c
ZC	crystalline	143	E-7				0.21	1.4	
ZC	SG ^b	250	E-7				0.29	1.1	
ZC	nematic	287	E-7				0.32	0.44	

^a The assignments of the RPs as singlet- or triplet-initiated is based on the phase of the signal (kinetics and spectra) and on the energy levels of the radical pairs. For the tri-exponential kinetics, $\tau_1 = \tau_{\text{RSRP}}$ (rise of the singlet-initiated RP), $\tau_2 = \tau_{\text{RTRP}}$ (rise of the triplet-initiated RP), and $\tau_3 = \tau_{\text{DRP}}$ (decay of the RP). For the bi-exponential kinetics, $\tau_1 = \tau_{\text{RT}}$ (rise of the photoexcited triplet ³ZCX) and $\tau_2 = \tau_{\text{DT}}$ (decay of the photoexcited triplet). All times are in μs . ^b Soft glass. ^c Phase inversion observed both in spectra and kinetics. ^d RP observed, but signal is too weak to accurately fit. ^e Phase inversion observed only in spectra.

of ³ZCPINI lies below that of ZC^{•+}–PI–NI^{•-}, confirming that the charge separation is not initiated at any time by ³ZCPINI (Table 4).

(b) Soft Glass and Nematic Phases. Upon increasing the temperature of E-7 into the soft glass phase, additional features are noticed in the TREPR spectra. The TREPR spectra at 240 K of photoexcited ZCPI and ZCNI are shown in Figure 4a. The spectra consist of two components, i.e., narrow signals, which are superimposed on broad ones. The broad spectra are attributed to the triplet excited state, ³ZCX, while the narrow ones are those of the RPs, which are generated via the routes shown in Figure 2. For ZCPI, only the broad spectrum attributed to the triplet ³ZCPI is observed, while a mixture of triplet and RP spectra are detected for ZCNI. Finally, only RP spectra are detected for ZCPINI (not shown). Additional features for the dyads are the absence of a correlation between the triplet decay and RP formation and the clear phase inversion observed in the RP spectra. Absorption/emission (a/e) → emission/absorption (e/a) occurs in the case of ZC^{•+}–NI^{•-} (Figure 4) and e/a → a/e occurs in the case of ZC^{•+}–PI–NI^{•-} (Table 4). As mentioned above, the phase inversion corresponds to the existence of two routes for producing the RP states, singlet-initiated accompanied by triplet-initiated. Therefore, the observed phase inversions clearly indicate that RP production follows the energy level diagram shown in Figure 3 (the kinetic analysis is discussed in detail in a later section). The opposite signs of the phase inversion in ZCNI vs ZCPINI are due to different spin polarization mechanisms (see below). Nevertheless, both molecules exhibit singlet-initiated spectra followed by triplet-initiated ones. The absence of a triplet spectrum in the case of ZCPINI is a consequence of the fact that ³ZCPINI is depleted rapidly to form the triplet-initiated charge-separated state.

Increasing the temperature of E-7 further to 250 K (just before the appearance of the nematic phase) results in further spectral changes (Figure 4b), which are in full agreement with the energy levels shown in Figure 3. At this temperature, ZCPI shows both triplet and RP spectra, which change phase relatively late in time. ZCNI exhibits less intense triplet spectra accompanied by RP spectra that change phase quite early in time. Finally, ZCPINI exhibits intense a/e RP spectra (not shown), which do not show any phase inversion. These observations imply that

as the triplet-initiated mechanism starts to dominate the spectra, the singlet-initiated spectra are short lived and in the case of ZCPINI the singlet-initiated RP is below the time resolution of the EPR experiment.

We attribute the appearance of triplet-initiated RPs in the soft glass phase to an increase in the solvent reorganization energy, λ_s , which allows the energies of the RP states to be tuned over a wide temperature interval.^{2,8,20–22} The change in the energies of the RPs can be quantified at those temperatures where some of the RPs show evidence for triplet initiation, while the other RPs at higher energies (less driving force) continue to show only the singlet-initiated RPs. This allows the solvation energies to be bracketed with an error no greater than the difference in the charge separation driving forces, when a triplet-initiated RP pair begins to be observed (Figure 3). For example, the triplet-initiated RPs of both ZC^{•+}–NI^{•-} and ZC^{•+}–PI–NI^{•-} are first observed at 240 K in E-7, which implies that the energy level of ZC^{•+}–NI^{•-} drops below that of ³ZCX (1.35 eV, Figure 3). Thus, a minimum energy level change for ZC^{•+}–NI^{•-} (and for all the RPs) in the 240 K soft glass relative to the crystalline phase, where $E_{\text{RP}} = 1.58$ eV for ZC^{•+}–NI^{•-}, is -0.23 eV. Also, the energy level change of the three RPs cannot be any greater than -0.5 eV, because this would result in triplet-initiated RP formation in ZCPI, which does not occur at 240 K (Figures 3 and 4). At 250 K the triplet-initiated TRP, i.e., ³[ZC^{•+}–PI^{•-}], is observed, now making -0.5 eV the minimum E_{RP} change at this temperature for the RPs. As a result, the reorganization energy of the soft glass at 250 K is already sufficient to produce E_{RP} values similar to those in the isotropic phase of E-7 (Table 3).

Increasing the temperature of E-7 so that it is in the nematic phase results in spectra that are practically the same as those observed in the upper limit of the soft glass regime. In terms of the energy-level diagrams (Figure 3), such a temperature change only slightly decreases the RP energies and does not significantly alter the singlet- and triplet-initiated RP production already observed in the soft glass. The TRP spectra of ³[ZC^{•+}–

(20) Heitele, H.; Finckh, P.; Weeren, S.; Pöllinger, F.; Michel-Beyerle, M. E. *J. Phys. Chem.* **1989**, *93*, 5173.

(21) Heitele, H. *Angew. Chem., Int. Ed. Engl.* **1993**, *32*, 359.

(22) Hasharoni, K.; Levanon, H.; von Gersdorff, J.; Kurreck, H.; Möbius, K. *J. Chem. Phys.* **1993**, *98*, 2916.

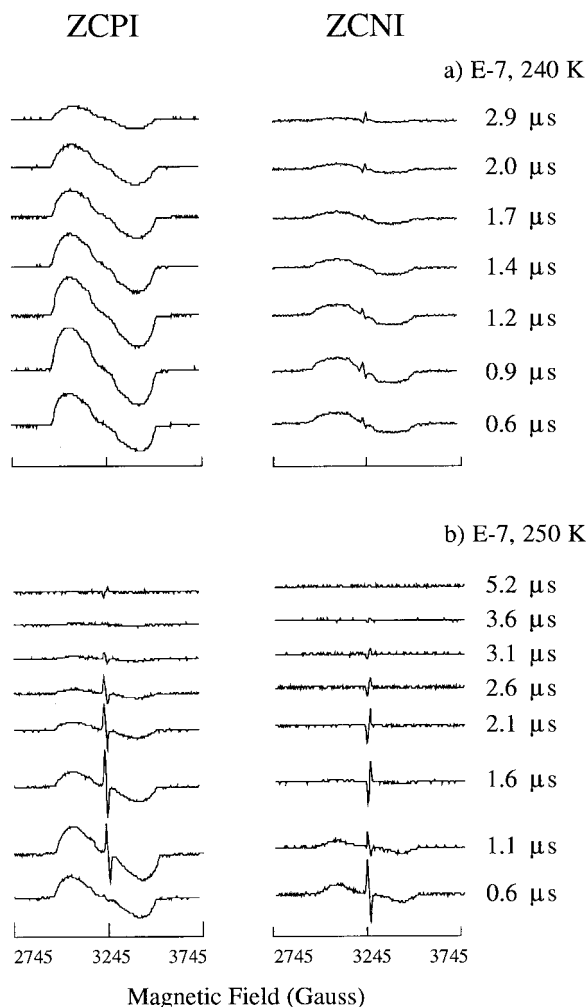


Figure 4. Direct-detection TREPR spectra (triplets and RPs), for different times after the laser pulse, of the photoexcited dyads in the soft glass of E-7 at: (a) 240 and (b) 250 K. The spectra clearly illustrate that the ZCPI radical pair has a lower driving force for charge separation because the radical pair is only evident at the higher temperature, whereas the radical pair of ZCNI is present at both temperatures. Furthermore, the spectra illustrate the large increase in the solvation ability of the soft glass, as only a 10 K increase in temperature produces a strong signal from the ZCPI radical pair.

$\text{PI}^{\bullet-}$] are in the a/e mode, indicating singlet-initiated spectra, which eventually change into triplet-initiated RPs, i.e., e/a at relatively late times (not shown). On the other hand, the TRP spectrum of $^3[\text{ZC}^{\bullet+}-\text{NI}^{\bullet-}]$ starts with an a/e pattern, which changes early in time into an e/a spectrum. In other words, both mechanisms are in operation for both dyads. Finally, the RP spectra of $\text{ZC}^{\bullet+}-\text{PI}-\text{NI}^{\bullet-}$ exhibit an a/e pattern, typical of a CRP spectrum that is initiated by the triplet precursor and is consistent with the large driving force from the photoexcited triplet of ZCPINI. The even higher driving force from the photoexcited singlet of ZCPINI results in a singlet-initiated CRP that is too short lived to observe by TREPR. To summarize the results in E-7, TREPR spectroscopy shows that the solvent reorganization energy in the upper limit of the soft glass is tuned to nearly that of the nematic (fluid) phase.

The maximum change of the energy levels of the RPs in the nematic phase can be determined independently by the following arguments. At 240 K we showed that the E_{RP} change from the crystalline phase for $\text{ZC}^{\bullet+}-\text{NI}^{\bullet-}$ ranged between -0.23 and -0.5 eV (i.e., E_{RP} equals 1.08 to 1.35 eV). However, in the nematic phase, the rate of charge separation of triplet-initiated

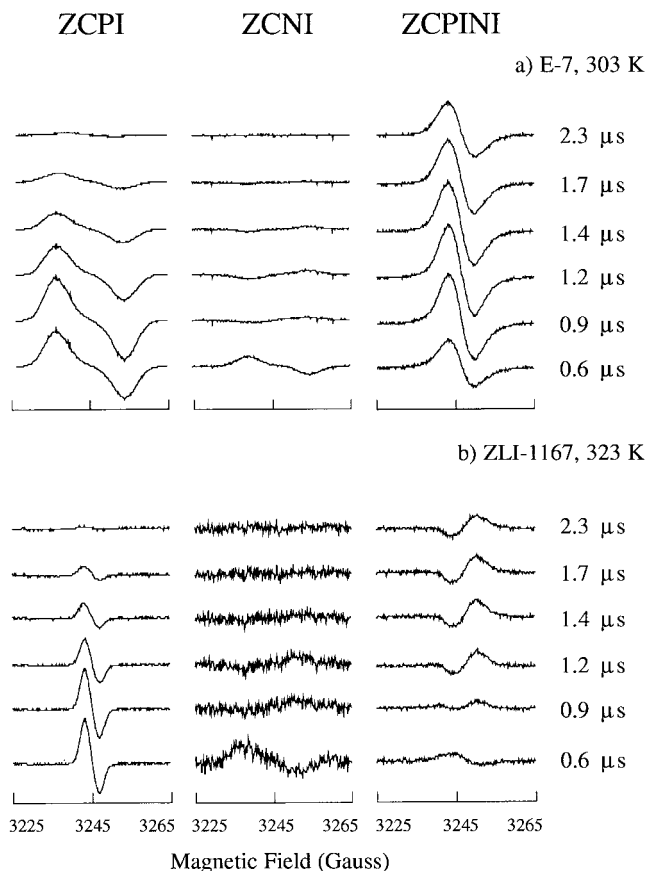


Figure 5. Direct-detection TREPR spectra (RPs), for different times after the laser pulse, of the photoexcited molecules in the nematic phase of (a) E-7 and (b) ZLI-1167.

$\text{ZC}^{\bullet+}-\text{PI}^{\bullet-}$ (Table 4) is the same as that for $\text{ZC}^{\bullet+}-\text{NI}^{\bullet-}$ at 240 K, implying that E_{RP} for $\text{ZC}^{\bullet+}-\text{PI}^{\bullet-}$ also ranges between 1.08 and 1.35 eV in the nematic phase. Note that because IET in LCs occurs in the adiabatic regime, the small electronic coupling differences between the molecules is of no significance.^{2,23,24} The average of this range is 1.22 eV, which agrees remarkably well with the 1.23 eV value calculated for $\text{ZC}^{\bullet+}-\text{PI}^{\bullet-}$ in the isotropic phase of E-7.

ZLI-1167 does not have a soft glass phase, but these arguments can also be extended to the smectic and nematic phases. The triplet-initiated RP $^3[\text{ZC}^{\bullet+}-\text{NI}^{\bullet-}]$ is first observed in the smectic phase at 299 K, again suggesting a minimum value for the change in RP energies from crystalline to smectic phases to be -0.23 eV, and the maximum value to be -0.5 eV. The triplet-initiated radical pair of $^3[\text{ZC}^{\bullet+}-\text{PI}^{\bullet-}]$ is first observed in the nematic phase at 323 K. It is clear that the triplet-initiated RPs are observed at higher temperatures in ZLI-1167 as compared to E-7. This can be explained by the lack of a soft glass phase in ZLI-1167. In this case, the smectic phase functions in a manner similar to the soft glass phase in E-7.

Triplet Radical Pair or Correlated Radical Pair Mechanisms. In terms of Figure 2, there are two possible mechanisms of IET to produce the RP states, i.e., the TRP and CRP mechanisms, that are consistent with the experimental observation of polarized EPR spectra (Figures 4 and 5). The formation of a TRP, such as $^3[\text{ZC}^{\bullet+}-\text{PI}^{\bullet-}]$, can be singlet and/or triplet initiated. Both cases were treated at length in previous papers.^{2,10,22} Since the present results agree with the earlier

(23) Rips, I.; Jortner, J. *Chem. Phys. Lett.* **1987**, *13*, 3411.

(24) Rips, I.; Jortner, J. *J. Chem. Phys.* **1987**, *87*, 2090.

analyses, we present only the final results here. The phase of the RP spectra differentiates between the two routes of RP production. Similar to previously studied systems, molecular modeling²⁵ shows that the plane defined by the π -systems in both PI and NI is not coplanar with that of ZC. Thus, for the case of a triplet precursor with an active Z-axis within the donor (ZC in our case), an e/a polarization of the TRP is expected. For the case of a singlet precursor, two sub-cases are possible. The first is S-T₀ mixing which produces an e/a polarization pattern, while the case of S-T₋₁ mixing produces an a/e pattern. Similar to other related systems,^{22,26} the relatively short donor-acceptor distances in ZC⁺-PI⁻ and ZC⁺-NI⁻ do not allow a vanishing J -value, thus S-T₋₁ mixing is the mechanism responsible for the polarization pattern observed for the singlet-initiated RP. Finally, it is important to note that the phase of the polarization pattern associated with a TRP spectrum (singlet or triplet initiated) does not change with the sign of $\Delta\chi$, i.e., E-7 vs ZLI-1167 (cf. Figure 5). However, the relative signal amplitudes can be varied in accordance with the different molecular alignment.¹⁴

The second mechanism is the correlated radical pair (CRP), where the two electron spins interact via the exchange (J) and dipolar (D) interactions in a four-level system.^{27,28} As with the TRP mechanism, the CRP spectral phases are essential to differentiate between the two possible precursors. The phase of the signal is determined by the CRP sign rule:²⁷

$$\Gamma = -\mu \text{sign}[J + D(3 \cos^2(\theta) - 1)] = \begin{cases} -a/e \\ +a/e \end{cases} \quad (3)$$

where D is the dipolar interaction strength, J is the exchange interaction strength, θ is the angle between the dipolar axis (z' in Figure 1) and the magnetic field direction, and μ is -1 or $+1$ for a singlet or triplet precursor, respectively. Thus, for $D < 0$ (as expected for the present RPs) and assuming that $J < 0$, the polarization pattern is e/a for the case of a singlet precursor ($\mu = -1$). For a triplet precursor ($\mu = +1$) the pattern is a/e. It is important to note that in E-7, the phase of the CRP signal for a particular precursor is reversed from that of the TRP. However, unlike the phase behavior for a TRP, the phase of the CRP signal inverts when ZLI-1167 is used, i.e., when $\mathbf{B} \perp \mathbf{L}$. The different polarization patterns in E-7 and ZLI-1167 are consistent with a CRP mechanism, in which the dipolar interaction is the main contribution.^{2,10,27,29-31} Thus, by analyzing the spectral line shape and by utilizing two different LCs, it is possible to distinguish between the TRP and the CRP mechanisms.

The relatively broad RP spectra of the dyads (ZC⁺-NI⁻ and ZC⁺-PI⁻), coupled with the absence of a phase change as a function of the LC used, indicate that these RPs exhibit the spectral characteristics of the TRP mechanism. These spectra were analyzed by employing the line shape formalism from which the magnetic and kinetic parameters were extracted (Tables 1 and 2). From the ZFS parameter, D , the donor-

acceptor distance can be estimated by using the dipole approximation:³²

$$D \approx \frac{3}{4} \frac{(g\beta)^2}{r^3} \approx \left(\frac{30}{r}\right)^3 \quad (4)$$

where r is the donor-acceptor distance. A value of $r = 11.5$ Å is obtained, in agreement with the known value of 11 Å. On the other hand, the RP spectral width of ZC⁺-PI⁻-NI⁻ is much narrower than those of the dyads (Figure 5) and exhibits phase inversion between the two LCs. A line shape analysis of the ZC⁺-PI⁻-NI⁻ spectra results in a ZFS parameter of $D = -8$ G, which produces a value of 15 Å for the donor-acceptor distance. However, this value is considerably shorter than the true value of 18 Å, indicating that the TRP mechanism is not valid for the triad RP spectra, thus confirming that the EPR spectra are governed by the CRP mechanism.

One intriguing difference in the spectra between the two dyads is noteworthy. In the fluid phase of ZLI-1167, ZCPI shows a conspicuously narrow RP spectrum as compared to that in E-7, unlike ZCNI or ZCPINI. Thus, at ~ 325 K, the peak-to-peak spectral widths are 16 G in E-7 and only 3.7 G in ZLI-1167. This compares to a 16 G width for ZCNI in both solvents, and a 6.5 G width for ZCPINI in both solvents. This unique feature is due to an additional dynamic effect of intermolecular triplet migration between neighboring molecules (two sites), which is allowed in ZLI-1167 for the less bulky ZCPI molecule. This effect was observed in other systems^{33,34} and does not interfere with the main theme of this paper.

Kinetic Data. The data and conclusions presented above are based on the spectral analysis of the different species formed under light excitation. The kinetic data are in full agreement with the mechanisms of charge separation and TREPR line shape. The corresponding data for the radical pairs ZC⁺-PI⁻-NI⁻, ZC⁺-PI⁻, and ZC⁺-NI⁻ in the nematic phases of E-7 and ZLI-1167 are shown in Figure 6. The kinetics were fit with the following fitting function:

$$M_y(t) = -A_1 e^{-(t-t_0)/\tau_1} + A_2 e^{-(t-t_0)/\tau_2} - A_3 e^{-(t-t_0)/\tau_3} \quad (5)$$

where t_0 is the time zero offset, τ_i ($i = 1-3$) are the exponential time constants for up to three rises and/or decays, and A_i ($i = 1-3$) are the corresponding amplitudes of the magnetization, $M_y(t)$. The formation and decay times of the triplet excited states and the triplet RPs in terms of τ_i are summarized in Table 4.

We first discuss the results for the dyads oriented in the two LCs. The kinetics of ZC⁺-PI⁻ and ZC⁺-NI⁻ exhibit the same behavior in the two LCs. While the former RP shows an exponential rise and decay, the latter dyad, whose RP energy is lower, exhibits a signal rise followed by an exponential decay and a phase change.³⁵ In terms of the discussion above, the single rise and decay curves are in agreement with singlet-initiated TRP production, while the complex kinetics indicate the existence of two routes operating simultaneously, i.e., the

(25) Hyperchem (Autodesk) molecular modeling software.

(26) Hasharoni, K.; Levanon, H.; Gätschmann, J.; Schubert, H.; Kurreck, H.; Möbius, K. *J. Phys. Chem. A* **1995**, *99*, 7514.

(27) Hore, P. J. In *Advanced EPR. Applications in Biology and Biochemistry*; Hoff, A. J., Ed.; Elsevier: Amsterdam, 1989; pp 405-440.

(28) Norris, J. R.; Morris, A. L.; Thurnauer, M. C.; Tang, J. *J. Chem. Phys.* **1990**, *92*, 4239.

(29) Tang, J.; Thurnauer, M. C.; Norris, J. R. *Chem. Phys. Lett.* **1994**, *219*, 283.

(30) Berman, A.; Izraeli, E. S.; Levanon, H.; Wang, B.; Sessler, J. L. *J. Am. Chem. Soc.* **1995**, *117*, 8252.

(31) Wasielewski, M. R.; Wiederrecht, G. P.; Svec, W.; Niemczyk, M. *P. Sol. Energy Mater. Sol. Cells* **1995**, *38*, 127.

(32) Expression 4 is based on the assumptions that the conjugation paths for the unpaired electrons are restricted to a flat moiety, where the expectation value of the ZFS parameter, D , is approximated into a two-dimensional frame of reference. For details, see ref 13 and refs 38 and 39 therein.

(33) Regev, A.; Galili, T.; Levanon, H. *J. Chem. Phys.* **1991**, *95*, 7907.

(34) Regev, A.; Galili, T.; Medforth, C. J.; Smith, K. M.; Barkigia, K. M.; Fajer, J.; Levanon, H. *J. Phys. Chem. A* **1994**, *98*, 2520.

(35) In some cases, phase inversion indicating a change from singlet-into triplet-initiated spectra is noticed only by the spectral line shape, and not by the kinetic traces. This occurs when the ratio between the two respective spectra exceeds the value of 1:5. In these cases the kinetic trace is dominated by the stronger component (see also Table 4).

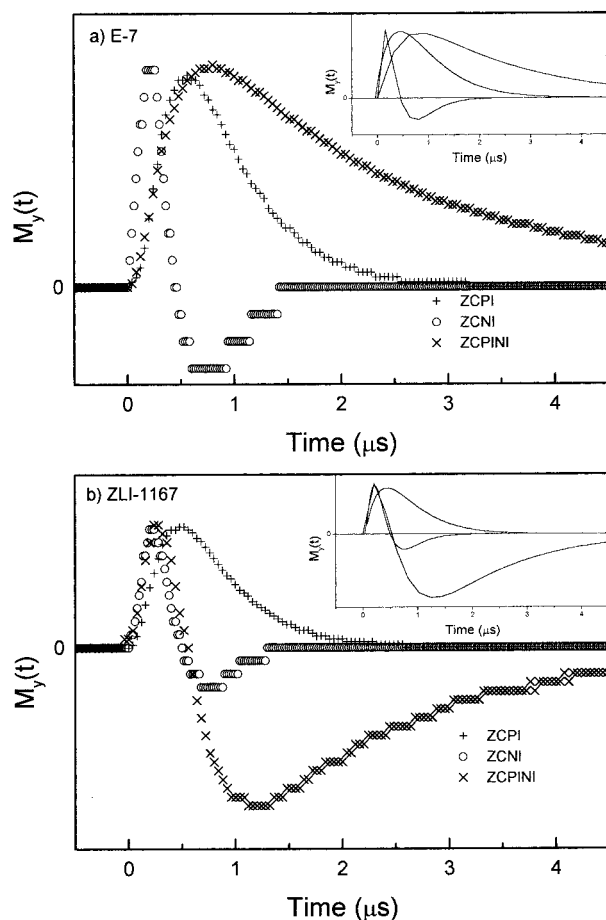


Figure 6. Kinetic traces of the RP formation and decay, taken at the low-field spectral range, for ZCPI, ZCNI, and ZCPINI in the nematic phase of (a) E-7 and (b) ZLI-1167. The insets show the fits to the data with eq 5.

fast rise is the singlet-initiated RP formation accompanied by the triplet-initiated route. The latter is dominant and shows up later in time. Under such conditions we cannot expect to observe a clear correlation between the triplet decay and the rise of the RP. The similar kinetics of the dyads in both LCs (except for the amplitudes) are in line with a TRP mechanism and with our previous assignment that the RP production of both dyads should have the same line shape and phase changes in the two different LCs. The TRP mechanism is also consistent with the donor–acceptor distances of ~ 11 Å in both dyads.

The triad RP ($\text{ZC}^{+\bullet}-\text{PI}-\text{NI}^{\bullet-}$) having the lowest energy exhibits kinetics in both LCs which show that the lifetime of the charge-separated state is much longer than those found for the dyad RPs. This is due to multistep charge separation. The kinetics in ZLI-1167 exhibits a phase change, reflecting the different routes of RP production. As discussed above, in accordance with the donor–acceptor distance of ~ 18 Å, the line shape of the triad RP should correspond to the CRP mechanism. In the case of E-7 the kinetics are straightforward and exhibit an exponential rise and decay, corresponding to an a/e pattern in the spectrum (Figure 5a), i.e., triplet-initiated CRP

production. This is also in line with the order of the energy states of the three molecules (Figure 3). In ZLI-1167 the kinetics exhibit a phase change, i.e., a \rightarrow e, which corresponds to a/e \rightarrow e/a in the spectrum (Figure 5b). In terms of eq 3 the RP signal in ZLI-1167 should be out-of-phase by $\pi/2$ as compared to E-7. Thus, as expected, the RP production corresponds to a singlet-initiated route, which is dominated by the triplet-initiated one at later times.

To summarize this part, it should be mentioned that our attempts to observe a triplet state generated via back electron transfer, similar to that found recently in a nonporphyrinoid system,^{9,10} failed. Thus, the back ET in our case couples the RP states with the ground-state singlet.

Conclusions

The TREPR data of the chlorophyll-like donor–acceptor systems permit quantitative analysis of the energy levels of the RPs in the crystalline/stiff glass, soft glass, and nematic phases of LCs. The radical pairs are destabilized by 0.6 ± 0.1 eV in the crystalline phase relative to the calculated energy levels for an RP in an isotropic, polar solvent. The soft glass phase of E-7 is remarkable in that nearly the entire energetic destabilization observed in the crystalline phase is recovered as the temperature is increased through the last 25 degrees of the soft glass phase. The nematic phase of E-7 shows very similar radical pair energies compared to the highest temperatures of the soft glass phase. The nematic phases of E-7 or ZLI-1167 show little destabilization relative to the calculations for an isotropic solvent of equivalent dielectric constant. The smectic phase of ZLI-1167 shows 0.2–0.5 eV of destabilization.

We have also demonstrated that the present photosynthetic model systems that employ single or multiple step charge separation have different mechanisms for creation of spin polarization in the RP. The dyads studied here exhibit a TRP mechanism, whereas the triad exhibits a CRP mechanism. As to what extent this may be a general conclusion for single-step vs multistep charge transfer is under study. Only TREPR in conjunction with LC alignment in a magnetic field allows differentiation between the two mechanisms. Moreover, such a combination allows a quantitative determination of the RP and the reorganization energies of donor–acceptor systems in these unique media.

Acknowledgment. We are indebted to Dr. Alexander Berg for his assistance, comments, and helpful suggestion in preparing this manuscript. The Farkas Center is supported by the Bundesministerium für Forschung und Technologie and the Minerva Gesellschaft für die Forschung GmbH. The research described herein was supported by grants from US-Israel BSF, Israel Council for Research and Development, by the Volkswagen Stiftung, and by the DFG (Sfb program 337). This work was also supported by the Division of Chemical Sciences, Office of Basic Energy Sciences, U.S. DOE under contract W-31-109-ENG-38.

JA980409C